REVIEW

doi:10.1038/nature10885

Functional complexity and regulation through RNA dynamics

Elizabeth A. Dethoff[1], Jeetender Chugh[1], Anthony M. Mustoe[1] & Hashim M. Al-Hashimi[1]

Changes to the conformation of coding and non-coding RNAs form the basis of elements of genetic regulation and provide an important source of complexity, which drives many of the fundamental processes of life. Although the structure of RNA is highly flexible, the underlying dynamics of RNA are robust and are limited to transitions between the few conformations that preserve favourable base-pairing and stacking interactions. The mechanisms by which cellular processes harness the intrinsic dynamic behaviour of RNA and use it within functionally productive pathways are complex. The versatile functions and ease by which it is integrated into a wide variety of genetic circuits and biochemical pathways suggests there is a general and fundamental role for RNA dynamics in cellular processes.

Analysis of the first X-ray structure of the protein myoglobin[1] prompted researchers to ask the question: how do ligands reach the deeply buried haem group centre? This simple, but powerful, observation has inspired decades of investigation into the dynamic behaviour of proteins, so that we now know protein structures are in constant motion, and that these fluctuations in structure are crucial to, and sometimes drive, function. Early X-ray structures of RNA contained indications of the importance of conformational dynamics: large changes in the helical arms of transfer RNA were observed on the binding of tRNA synthetase[2], and changes in the conformation of ribozymes needed to be invoked to envision catalytically active states[3–5]. However, no one could have anticipated the existence of new genetic circuits that are based on RNA conformational switches, or that the 'acrobatic' nature of a biopolymer that consists of only four chemically similar nucleotides would be at the centre of a complex macromolecular structure such as the ribosome.

The dynamic changes that occur in the structure of RNA serve an ever-increasing range of functionality that generally follows a common two-step process (see Supplementary Information for more reviews on RNA dynamics). The process involves a cellular signal that triggers RNA dynamics, which are then transduced into a specific biological output. This Review provides a critical account of RNA dynamics as a regulatory mechanism and source of functional complexity. We review the known dynamic properties of RNA structure and emphasize the unique properties that allow large changes in structure to take place in a biologically specific and robust manner. We then examine the wide range of cellular inputs used to interface with RNA dynamics and the various mechanisms that are used to guide the dynamics to achieve a broad spectrum of functional outputs.

RNA free-energy landscape

It is important to distinguish between the two types of RNA dynamics: 'equilibrium fluctuations' and 'conformational transitions'. Equilibrium fluctuations are related to the thermal activated motions that occur in RNA. Conformational transitions arise when cellular cues, such as an increase in the concentration of a metabolite, create a non-equilibrium state that then relaxes back to equilibrium. This Review is focused principally on conformational transitions because of their dominant role in regulatory mechanisms; however, the two motions are intricately related, as highlighted by studies of RNA and protein dynamics[6,7]. This, and other aspects of RNA dynamic behaviour that are relevant to function, is best understood by looking at the free-energy landscape of RNA[8,9].

The free-energy landscape specifies the free energy of every possible RNA conformation (Fig. 1a). Equilibrium fluctuations correspond to the spontaneous jumps that occur between various conformers along the free-energy landscape. The population of a given conformer depends on its free energy, whereas the transition rate between conformers depends on the free-energy barrier of separation (Fig. 1a). Conformational transitions arise when cellular cues perturb the free-energy landscape, which leads to a redistribution of conformational states (Fig. 1a). The RNA free-energy landscape is punctuated by deep local minima, or conformational wells, in which conformations within a well are highly similar and conformations from different wells are structurally distinct. These are the conformations that are significantly sampled by equilibrium motions and are stabilized by cellular cues to effect conformational transitions[10–12] (Fig. 1a). For example, the degeneracy of base-pairing and stacking interactions, together with the high stability of RNA duplexes, results in deep local minima that correspond to different but energetically equal secondary structures that are separated by large kinetic barriers[13] (Fig. 1b). As few as two secondary structures can dominate the RNA dynamic landscape because the loss of energy that accompanies the disruption of just one base-pair can markedly destabilize alternative conformations. In addition, RNA of a given secondary structure can undergo more facile dynamic excursions in tertiary structure, which involve smaller energetic barriers. These dynamics are commonly dominated by large changes in the relative orientation of helical domains, which carry motifs involved in tertiary contacts, and occur around flexible pivot points consisting of bulges, internal loops and higher-order junctions (Fig. 1c).

Although these excursions can lead to very large changes in tertiary structure, they are limited to a narrow set of conformations. For example, calculating the set of conformations that are accessible to two helices that are connected by a three-residue bulge reveals that the interhelical bend angle, when combined with interhelical twisting, can range from 0° to 180°. Despite this large accessible range, the connectivity constraints that are imposed by the bulge junction and the steric forces that act on the two helices direct changes in the interhelical orientations along a highly directional pathway and therefore restrict the conformational space to less than 20% of what

[1]Department of Chemistry and Biophysics, The University of Michigan, 930 North University Avenue, Ann Arbor, Michigan 48109-1055, USA.

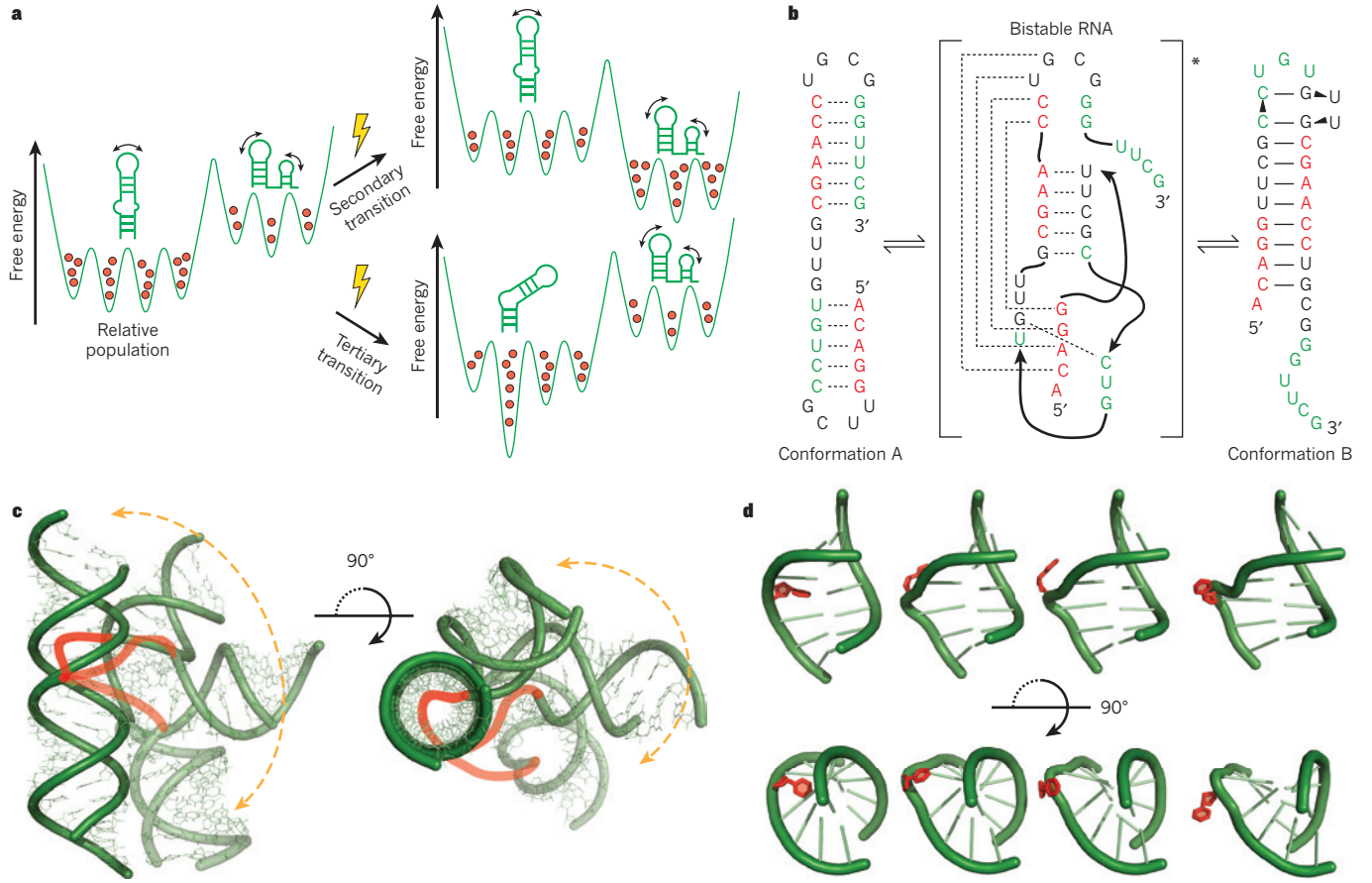

Figure 1 | Shape and form of RNA dynamics. **a**, The secondary and tertiary RNA conformations of different low-lying energy states are shown above the RNA free-energy landscape (green line). The relative populations of each conformation are shown within the landscape (red balls). Cellular effectors (bolts) can modify the energy landscape to favour an alternative secondary structure (top), or preferentially stabilize an alternate tertiary conformation (bottom). **b**, Exchange between alternative, isoenergetic secondary structures (A and B) that are separated by large energetic barriers owing to disruption of base pairs in the transition state[13]. **c**, The accessible range of interhelical conformations for an RNA two-way junction consisting of a trinucleotide bulge, with the possible paths of the bulge, which were excluded during the modelling, illustrated in red[14,15]. The allowed range of conformations is restricted towards a specific and directed conformational pathway by steric and stereochemical forces. The structure is rotated 90° to illustrate the bending (left) and twisting (right) motion. **d**, Flipping out of a residue (red) participating in a non-canonical base pair within an RNA internal loop is illustrated, progressing from an intrahelical stacked to an extrahelical unstacked conformation. The motion occurs without perturbing flanking Watson–Crick pairs (green).

is theoretically possible[10,14–16] (Fig. 1c). In addition, owing to the high stability of duplexes, residues participating in non-canonical base pairs can loop-out from intra- to extrahelical conformations without significantly disturbing the structure of the flanking helices[17,18] (Fig. 1d). Precise control over these dynamics is encoded within the sequence, and small sequence variations can greatly alter the relative populations of different RNA structures and their rates of interconversion[11,19]. For example, distinct interhelical orientations can be sampled by changing the length and asymmetry of junctions[10,14,15], and the tendency of residues to loop-out can be modulated on the basis of sequence-specific stacking interactions[20,21] (see Supplementary Information for links to movies and animations of experimentally determined RNA dynamics).

These features can help to explain the three remarkable aspects of RNA conformational transitions that are of fundamental importance for regulatory functions. First, the landscape is hierarchical due to the height of the energy barriers that separate alternative secondary structures. Changes in tertiary contacts rarely involve changes in the secondary structure and the two types of conformational changes can be used to serve different functions. Throughout this review, we will use 'secondary' and 'tertiary' conformational changes to distinguish between these two types of dynamics. Second, the limited landscape of energetically favourable conformations allows RNA to undergo very large changes in structure, but to be directed towards a very specific set of conformations from a vast number of possibilities. Third, there is increasing evidence that RNA dynamics are determined by the underlying RNA free-energy landscape, and to lesser extent by cellular cues[7,22,23]. Thus, conformational transitions can be considered perturbations that guide pre-existing equilibrium fluctuations towards specific functionally productive pathways. In this way, even an imperfect force or cellular signal will drive changes in the RNA structure along a predetermined pathway, which makes the transitions highly robust.

Triggers of RNA conformational transitions

RNA dynamics can be triggered by a remarkably diverse set of molecular effectors and environmental cues through several different mechanisms. This provides many different points of entry for integrating RNA conformational transitions into biological circuits and biochemical pathways.

Specific protein binders

The most common effectors are proteins that bind their target RNA specifically through well-defined structural features, thereby stabilizing one or a subset of conformations from the pre-existing energy landscape. For example, the mitochondrial tyrosyl-tRNA synthetase CYT-18 from *Neurospora crassa* binds specifically to group-I introns (a class of large self-splicing ribozymes that catalyse their own excision from messenger RNA, tRNA and ribosomal RNA precursors) and stabilizes the conformation required for catalytic activity[24]. Protein binding often leads to large changes in the overall orientation of RNA helices around

junctions such as bulges[25], three-way junctions[26] and other motifs such as the K-turn[27]. For example, the spliceosomal U4 small nuclear RNA (snRNA) undergoes a sharp transition in the interhelical bend angle, from approximately 69° to 25°, around a K-turn motif, when it binds to its cognate protein target[28] (Fig. 2a). These changes in interhelical conformation are driven in part by nonspecific electrostatic interactions between basic amino acids and the high negative-charge density that builds up at interhelical junctions, and are often observed as equilibrium dynamics in the absence of an effector[29–31]. For example, unbound HIV-1 transactivating response RNA (TAR) dynamically samples the many different interhelical orientations that are observed when it is bound to seven distinct ligands, including peptide mimics of its cognate protein, Tat[31] (Fig. 2b).

In an increasing number of cases, protein binding does not involve the stabilization of a specific minimum of the RNA free-energy landscape. Instead, binding selectively lowers the surrounding energy barriers to accentuate or alter the equilibrium dynamics of the RNA. For example, binding of the U1A protein to its cognate RNA target does not cause the pre-existing equilibrium interhelical motions to stop, but rather induces mobility in regions of the RNA that are in direct contact with the protein[32]. The CBP2 protein from yeast mitochondria binds specifically to the bI5 group-I intron and activates large-scale RNA equilibrium motions[33]. Even simple small-molecule ligands lead to the reorganization of the TAR RNA equilibrium dynamics[34]. These observations highlight the importance of embracing a broader view of trigger factors as elements that perturb the entire energy landscape and guide RNA dynamics rather than simply stabilize a single conformation from a dynamic range.

RNA chaperones and helicases

As is often the case in RNAs that possess alternative secondary structures, the large energy barriers associated with base-pair melting can limit the dynamics between RNA conformational wells. In this way, the RNA can become kinetically trapped in a metastable, non-equilibrium conformation. In response to this, a variety of proteins have evolved that possess the RNA 'chaperone' activity needed to efficiently drive RNA secondary structural-transitions over the large energy barriers[35,36]. For example, the HIV nucleocapsid protein uses non-specific interactions between the RNA and protein to destabilize the RNA helices[37]. This lowers the energetic barrier to conformational exchange, accelerating relaxation to equilibrium and allowing metastable RNAs to convert to conformations that are more thermodynamically favourable.

Other RNA chaperones, such as RNA helicases, help RNA traverse high energy barriers by unwinding helices and disrupting RNA structure, as well as promoting the formation of new RNA duplexes to accelerate conformational transitions in RNAs and ribonucleoprotein (RNP)

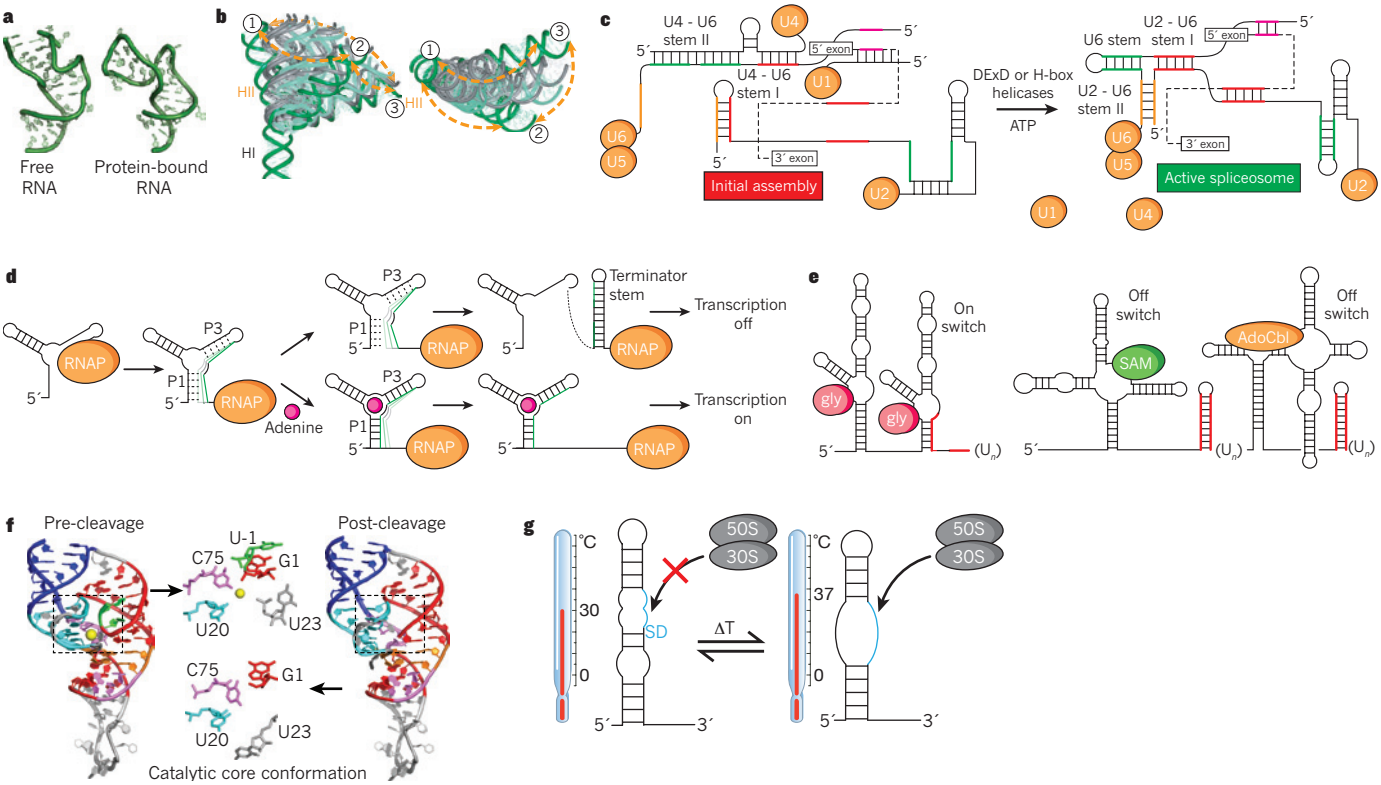

Figure 2 | Triggering RNA conformational transitions. **a**, Conformational changes in the spliceosomal U4 snRNA K-turn motif (Protein Data Bank (PDB) ID 2KR8) triggered when it binds to a complex of the human protein PRP31 and the 15.5K protein (PDB ID 2OZB)[28]. **b**, Similarity between the TAR RNA interhelical conformations that are triggered by binding to small molecules, Tat peptide derivatives and divalent ions (grey helices) and those that are sampled by equilibrium dynamics (green helices labelled as 1,2 and 3) in the unbound state shown as a horizontal and vertical view. The path of helix II (HII) as it moves from one unbound, equilibrium conformer to the next is shown by the orange arrows. HI, helix 1. Figure modified, with permission, from ref. 31. **c**, RNA conformation transitions during spliceosome assembly on pre-mRNA (dashed line) in the presence of DExD or H-box helicases and ATP. Sections are colour-coded to indicate base-pairing after helicase action. **d**, The RNA structure is modulated by steering of the co-transcriptional folding pathway. The adenine transcription-terminating riboswitch is a typical example. The progression of co-transcriptional folding with and without the ligand (adenine) is shown. Adenine binds to the apatamer domain and stabilizes the structure, allowing transcription to be turned on. RNAP, RNA polymerase. **e**, Two examples of tandem riboswitch architectures. Left, cooperative binding of glycine by the glycine riboswitch using tandem aptamer domains and one expression platform. Right, tandem SAM and AdoCbl riboswitches in which either of the two ligands triggers the conformational switch and yields an output of gene repression. Sequences that can form transcription terminator stems are shown in red. **f**, Conformations of HDV ribozyme pre-cleavage (PDB ID 1VC7)[53] and post-cleavage (PDB ID 1DRZ)[52] states. Enlarged details of the catalytic core (dashed box) of the two structures are shown, with the bound substrate (green) and the magnesium ion (yellow) present only in the pre-cleavage state. **g**, Melting of the secondary structure around the ribosome-binding site of virulence genes in the pathogen is triggered by an increase in temperature that makes the Shine-Dalgarno sequence (SD, blue) available for ribosome binding and translation initiation.

complexes[38]. These chaperone proteins are important for remodelling the structure of RNA and RNP complexes because they can anneal or unwind RNA strands depending on the environmental cues[39]. For example, helicases are essential in the assembly of the spliceosome, which is a complex RNP that consists of five RNAs and multiple proteins that catalyses excision of introns from a nuclear pre-mRNA[40,41]. Assembly proceeds through a series of transitions that involve the melting and annealing of RNA duplexes that are catalysed by DExD/H-box ATPase helicases (Fig. 2c). For example, the U4 RNA escorts the U4–U6–U5 triple small nuclear RNP complex (tri-snRNP) to the pre-mRNA, but is subsequently released by the DExD/H-box helicase Brr2, which catalyses the melting of the two stems within U4 and U6. This frees the U6 stem to base-pair with U2 snRNA and leads to a new RNA structure that is required for the first transesterification reaction[42] (Fig. 2c). In addition, DExD/H-box proteins are involved in the release of mRNA produced in pre-mRNA splicing reactions. For example, the DEAH-box splicing factor Prp22 is deposited on spliced mRNA downstream of the exon–exon junction and catalyses the disruption of contacts between mRNA and U5 snRNP, thereby releasing the spliced mRNA from the U5–U6–U2 spliceosomal assembly[43]. In another example of the variety of functions of RNA chaperones, the DExD/H-box protein CYT-19 unfolds native and misfolded conformations of a group-I catalytic RNA in an ATP-dependent process. A large free-energy gap between the native and misfolded conformers directs CYT-19 to unfold misfolded conformers more frequently than native conformers. In the process, CYT-19 redistributes the two conformation populations, which allows native RNA to populate a wider range of conformations than would otherwise be possible[44].

Metabolites and physiochemical conditions

Another ingenious strategy is used to modulate RNA structure in response to a wide range of metabolite-based effectors, including small molecules (such as amino-acids, coenzymes and nucleotides[23,45]) and changes in physiochemical conditions (such as magnesium ion concentration[46] and pH[47]). It would be difficult, if not impossible, for these smaller effectors and cellular cues to possess the chaperone activity needed to efficiently drive secondary structural transitions over the associated large energy barriers. Instead, this strategy operates on the initial RNA-folding process itself, intervening while the energy barriers are still low. Specifically, these effectors and cues act by directing the RNA to different folding pathways during RNA co-transcriptional folding. This process is made possible by the unidirectional and comparatively slow rate with which RNA is transcribed from the 5′ to the 3′ direction relative to RNA folding and effector binding. Each pathway favours one of two distinct secondary structures, where each secondary structure is associated with an alternative biological outcome (Fig. 2d). This trigger mechanism is implicated in a growing list of other RNA switches, although it has been best described for metabolite-sensing riboswitches[23,45].

Riboswitches are RNA-based genetic elements typically embedded in the 5′ untranslated region of bacterial genes that regulate expression of metabolic genes in response to changes in cellular metabolite concentration[23,45]. In a prototypical metabolite riboswitch, a metabolite, such as adenine, binds to the aptamer domain with exceptional affinity and selectivity. This stabilizes an otherwise shallow energy well, which induces a redistribution of the aptamer conformational states towards one state that, in most riboswitches, sequesters an RNA element into a helix of the aptamer domain[48] (Fig. 2d). In turn, the unavailability of the RNA element changes the folding pathway of a downstream decision-making expression platform, directing it towards structures that turn off (and in some cases, turn on) gene expression, either by forming a transcription-terminating helix (Fig. 2d) or by sequestering the Shine-Dalgarno sequence (a ribosome binding site located eight base pairs upstream of the start codon in mRNA), thereby inhibiting translation. This system also keeps the number of spontaneous conformational transitions, or premature switching in the absence of ligands, to a minimum because very large energy barriers separate the two alternative secondary structural forms of the expression platform.

More complex functionality can be achieved by coupling multiple riboswitches together. For example, the glycine riboswitch uses two aptamer domains in tandem to cooperatively bind glycine, thereby increasing responsiveness to changes in ligand concentrations[49] (Fig. 2e). The tandem arrangement of two entire riboswitches that respond to two distinct ligands allows the construction of more sophisticated genetic circuits such as two-input Boolean NOR logic gates, in which either of the two ligands can trigger the conformational switch and yield an output of gene repression[50] (Fig. 2e). In another example, the c-di-GMP-sensing riboswitch and a GTP-dependent self-splicing group-I ribozyme in the 5′ untranslated region of a putative *Clostridium difficile* virulence gene work in tandem to regulate translation[51]. In the presence of c-di-GMP and GTP, the riboswitch and ribozyme form a structure that stabilizes a 5′ splice site, and the ribozyme self-splices to yield an RNA transcript with a perfect ribosome-binding site located upstream of the start codon. Conversely, in the presence of GTP alone, alternative base pairing between the riboswitch and ribozyme occurs to form a structure that promotes splicing at an alternative site, which results in a splicing product without a ribosome-binding site, and thus downregulates translation. This RNA arrangement represents the first natural example of an allosteric ribozyme.

Chemical reactions

Chemical reactions, such as cleavage of the RNA phosphodiester backbone, can also reshape the underlying RNA energy landscape so that a state that was previously in equilibrium becomes a non-equilibrium state, which triggers changes in RNA secondary and tertiary structure. For example, X-ray analysis of the structures of precursor and product states of the hepatitis delta virus (HDV) ribozyme, which catalyses site-specific self-cleavage of the viral RNA phosphodiester backbone, reveal changes in the local arrangement of catalytic groups, as well as the ejection of a catalytically important magnesium ion[52]. These conformational changes may help to accelerate product release[53,54] (Fig. 2f). Another example is seen in the secondary structural switch triggered by cleavage of the 3′ end of the pre-18S rRNA during eukaryotic ribosome maturation, which is used to enforce a sequential order to the maturation process[55].

Thermal and mechanical triggers

Other energy-dependent processes can induce the complete 'melting' of RNA helices. RNA thermosensors alter expression of genes during heat-shock response and pathogenic invasion in response to increases in temperature[56] (Fig. 2g). For example, when *Listeria monocytogenes* invades an animal host, the pathogen enters a warmer environment, which activates a thermosensor located at the 5′ untranslated region of the *prfA* mRNA[57]. The higher host temperature causes a shift in the energy landscape from one that favours the formation of the thermosensor hairpin to one that favours the melted, single-stranded conformation. This melting transition exposes ribosome-binding sites, which are required for translation. Mechanical triggers can also induce the unfolding of RNA hairpins. One example is translation-induced unfolding of mRNA hairpins, which is thought to slow the rate of ribosome elongation to allow the folding of autonomous-folding proteins and protein domains[58].

Functions of secondary structural transitions

Secondary structural transitions are widely used in gene regulation as binary switches that are activated by cellular cues. The switch can be transduced into a range of outputs by sequestering or exposing key RNA regulatory elements.

Transcription

Many RNA switches regulate gene expression at the transcriptional level by producing transcription-terminating helices. In addition to metabolite-sensing riboswitches, other RNA switches use the same strategy to regulate gene expression in response to more complex molecules[23,45]. For example, in the T-box mechanism,

non-aminoacylated or uncharged tRNA can activate transcription of the cognate gene that encodes its aminoacyl-tRNA synthetase. The interaction between the acceptor end of an uncharged tRNA and residues in the antiterminator bulge in the 5′ untranslated region of the mRNA (Fig. 3a) promotes formation of an antiterminator helix during co-transcriptional folding that allows transcription to continue. However, the acceptor end of aminoacylated or charged tRNA cannot interact with the antiterminator helix residues, which results in formation of the more stable terminator stem that aborts synthetase gene transcription[59] (Fig. 3a). Only a few proteins have been identified that modulate transcription by influencing folding of transcription-terminating helices. One example is the tryptophan-activated RNA-binding attenuation protein (TRAP), which binds *trp* mRNA to regulate gene expression at both the transcriptional and translational level by several processes (for example, promoting the formation of a terminator hairpin that terminates transcription[60]).

Translation

There is an increasing list of protein- and RNA-triggered[61] RNA switches that regulate translation by sequestering or exposing ribosome-binding sites or by affecting the structure of ribosomal RNA, and therefore blocking translation. For example, a protein-dependent RNA switch has recently been identified in the 3′ untranslated region of *VEGFA* mRNA in myeloid cells that regulates translation of *VEGFA* in response to proteins associated with two disparate stress stimuli (Fig. 3b). The interferon-γ (IFN-γ)-activated inhibitor of translation (GAIT)-complex binds a structural GAIT element within a family of inflammatory mRNAs and silences their translation by promoting the formation of a translational-silencing (TS) conformer[62]. During oxidative stress, the heterogeneous nuclear ribonucleoprotein L (hnRNP L) overrides GAIT silencing by triggering a secondary structural RNA switch to a translation-permissive (TP) conformer, in which the GAIT element is occluded. The RNA alternates between two mutually-exclusive conformers in response to the binding of the GAIT complex or hnRNP L, thereby functioning as an AND NOT Boolean logic-gate switch in which the presence of one protein, but not the other, yields an output of gene repression (Fig. 3b).

Post-transcriptional processing

An increasing number of RNA switches are involved in regulating post-transcriptional processing; for example, splicing, gene silencing by microRNA (miRNA) and RNA editing. Although the detailed mechanics of many of these systems are still unknown, in all cases the RNA switch exposes, occludes or modulates the structure of the processing sites to regulate post-transcriptional processes. For example, one of the thiamine pyrophosphate riboswitches discovered in eukaryotes

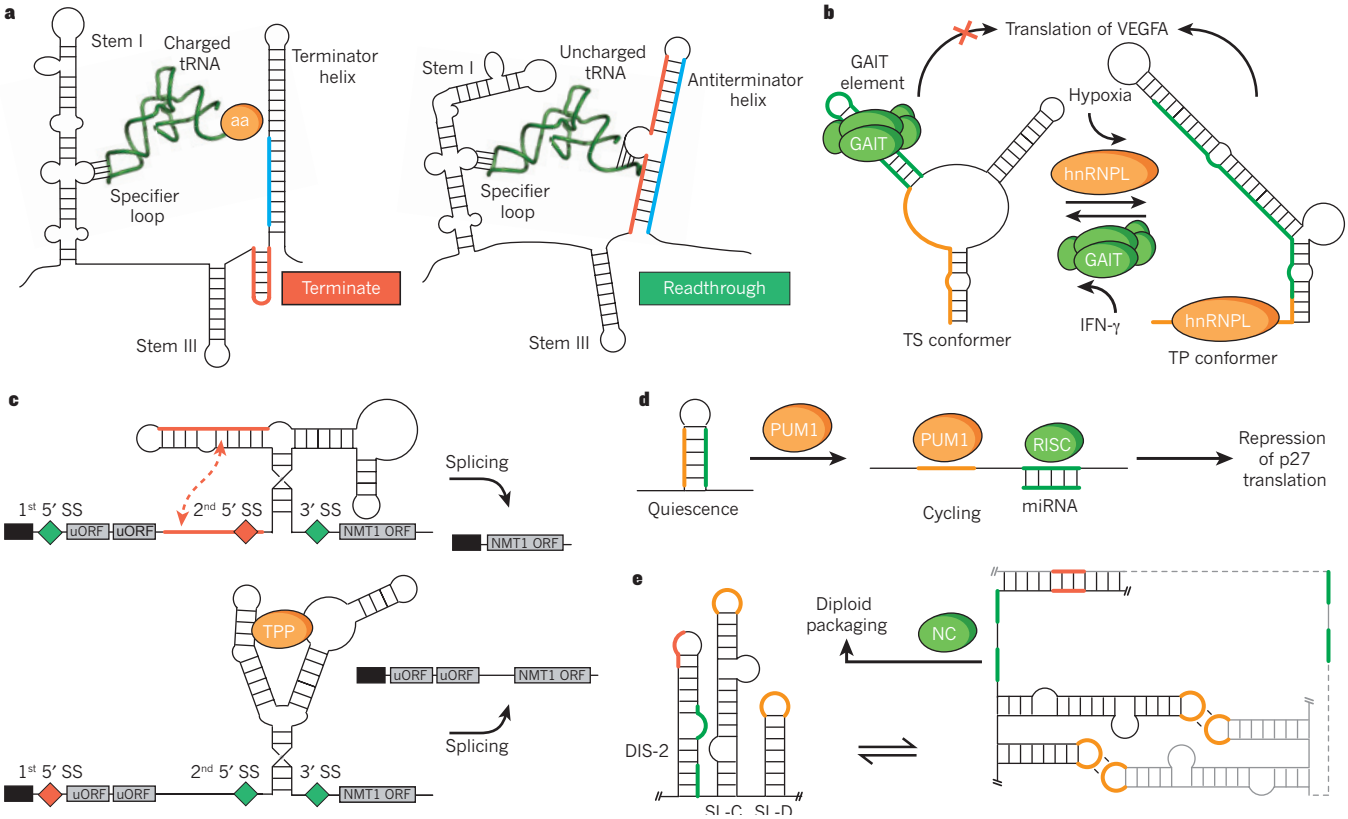

Figure 3 | Functional outputs of secondary structural changes. **a**, Transcriptional activation of the aminoacyl-tRNA synthetase gene by uncharged tRNA (no aminoacylation (aa)). Binding of uncharged tRNA induces formation of an antiterminator helix during co-transcriptional folding[99]. **b**, Translation control of *VEGFA* expression through a dual protein-dependent RNA secondary structural switch that responds to interferon-γ (IFN-γ) by binding the IFN-γ-activated inhibitor of translation (GAIT) complex (green) to form a translational-silencing (TS) conformer (on the left) and to hypoxic stress that results in hnRNP L binding and causes a switch to a translation permissive (TP) conformer (on the right). **c**, Thiamine pyrophosphate (TPP) riboswitch-regulated alternative splicing and gene expression of NMT1. In the absence of TPP, the aptamer domain base-pairs (red dotted line) to the sequence surrounding a proximal 5′ splice site (SS, shown as coloured diamonds: green, activation or red, repression) to block it from the SS machinery. Instead, a distal SS is selected. On binding TPP, the aptamer domain undergoes a conformational change to expose the second proximal 5′ SS. The resultant spliced mRNA contains decoy upstream open reading frames (uORFs), thus reducing expression of the NMT1 ORF. **d**, Pumilio protein-mediated mRNA secondary structural switch controls accessibility of microRNA-binding sites and regulates expression of p27 protein. Binding of PUM1 induces a conformational change to expose the miR-211 and miR-222 binding site to allow p27 silencing. RISC, RNA-induced silencing complex. **e**, Secondary structural switch couples dimerization and diploid genome packaging of the Moloney murine leukaemia virus. Dimerization leads to a coupled frame-shift that exposes nucleocapsid protein binding sites (green) required for genome packaging. NC, nucleocapsid.

regulates alternative splicing[63] (Fig. 3c). Here, changes in the secondary structure sequester or expose splice sites (Fig. 3c). An RNA switch has recently been identified in the 3′ untranslated region of p27 mRNA that simultaneously sequesters both an miRNA target site from cleavage by the RNA-induced silencing complex (RISC) and a Pumilio-recognition element (PRE), which binds a Pumilio RNA-binding protein (PUM1)[64]. Binding of PUM1 to the PRE region triggers a secondary structural switch that exposes the miRNA target site, leading to miRNA silencing (Fig. 3d). In another example, HDV genotype III editing levels are determined by a pre-existing equilibrium between two secondary structures of the antigenome RNA, involving a kinetically trapped conformation and a thermodynamically more favourable state[65]. These initial discoveries suggest RNA switches have a range of functions in post-transcriptional processing.

Viral replication

RNA genomes of retroviruses take advantage of RNA secondary structural switches to transition between the different functions required for the various steps of the viral replication cycle. For example, there is evidence that the 5′ untranslated region of the HIV-1 genome can form two mutually exclusive secondary structures: a metastable branched multiple-hairpin conformation, which is involved in dimerization and packaging; and a more energetically favourable long-distance interaction conformation, which is involved in transcription and translation. The transition from the long-distance interaction to the branched multiple hairpin conformation is catalysed by the RNA chaperone nucleocapsid protein[66].

RNA switches can also couple distinct processes within a given step. For example, an RNA switch is used to couple dimerization and selective encapsidation of two copies of the Moloney murine leukaemia virus RNA genome. Dimerization of two RNA genomes induces a shift in the base-pairing pattern within the ψ-RNA packaging signal, which exposes conserved UCUG elements that bind the nucleocapsid protein with high affinity, thereby promoting genome packaging[67] (Fig. 3e). These elements are base-paired and bind nucleocapsid protein weakly in the monomeric RNA (Fig. 3e).

Functions of tertiary conformational changes

RNA tertiary conformational changes can range from large global changes in the orientation of helices to more subtle local changes in the structure of motifs that are involved in tertiary interactions. These conformational transitions allow RNA molecules to bind adaptively to a wide range of molecular partners and can help to direct the assembly of RNPs.

Polyvalent binding

Some of the first solved structures of RNA–protein complexes revealed a remarkable ability of RNA to undergo adaptive changes in conformation[2,25] that had the potential to allow the optimization of intermolecular interactions with disparate targets. In a classic example, these conformational changes allow tRNAs to interact with many diverse partners, including ribonuclease P (RNase P), various nucleotide modifying enzymes, tRNA synthetase, EF-Tu, the ribosome and other RNA elements. High-resolution structures of tRNA, tRNA–protein and

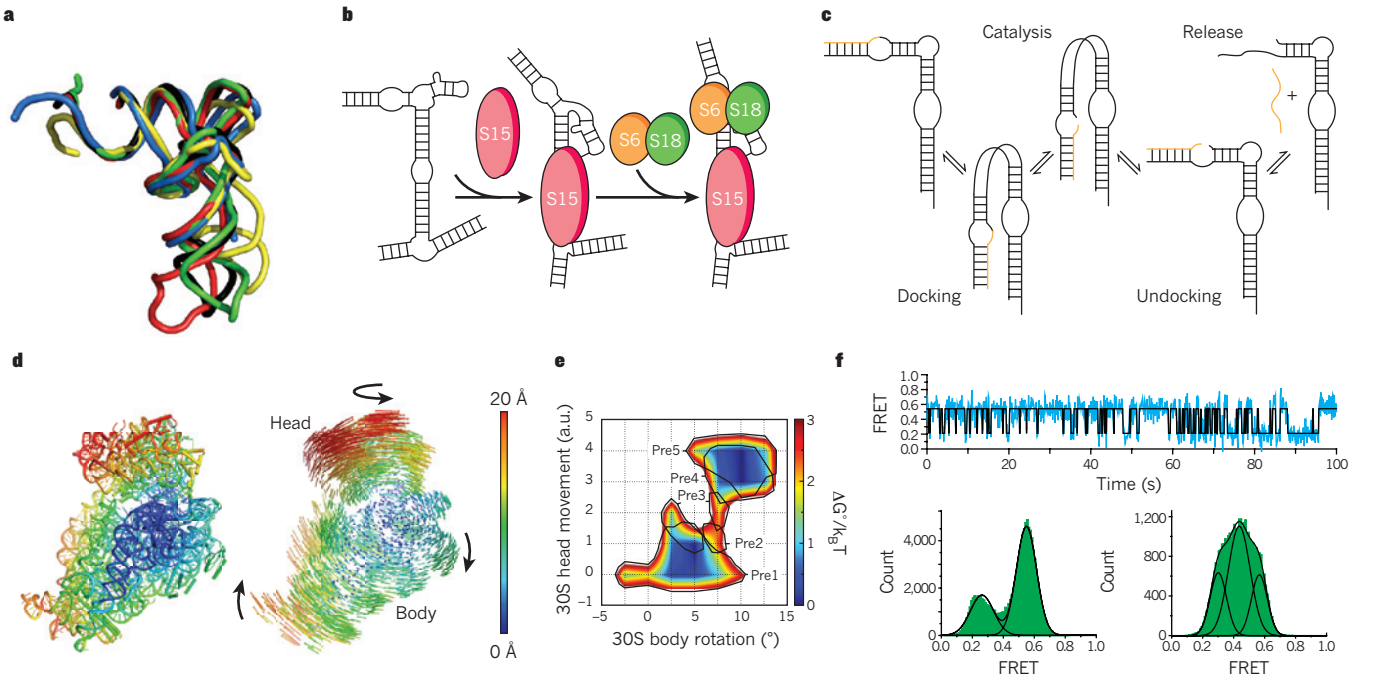

Figure 4 | Functional outputs of tertiary conformational changes. **a**, Different X-ray structures of $tRNA^{Phe}$ in the unbound state (black, PDB ID 1EHZ), in complex with RNaseP (blue, engineered anticodon stem removed, PDB ID 3Q1Q), the ribosome in the P/E state (green, PDB ID 3R8N), isopentenyl-tRNA transferase (red, PDB ID 3FOZ), and phenyalanyl-tRNA synthetase (yellow, PDB ID 1EIY). The structures are superimposed by the acceptor stem. **b**, Hierarchical assembly of the central domain of the 30S ribosomal subunit by successive protein-induced changes in the conformation of 16S rRNA. S15 changes the orientation of the helical domains to favour the binding of S6 and S18. **c**, Enzymatic cycle of the hairpin ribozyme. **d**, Ratcheting motions of the ribosome seen through X-ray crystallography. The degree of 30S subunit atomic displacement between the unratcheted and R_2 ratcheted states with the 50S subunit as a reference (not shown) are colour-coded by Å. Atomic displacement vectors and arrows (on the right) indicate the direction of the change. Figure reprinted, with permission, from ref. 82. **e**, The free-energy landscape of ribosomal ratcheting, as calculated from subclassification of cryoelectron microscopy particles. Movements of the 30S subunit body and head domains in relation to the 50S subunit are shown in units of degrees and arbitrary units (a.u.), respectively, with corresponding tRNA translocation intermediates (Pre1 and so on) outlined in black. Figure reprinted, with permission, from ref. 84. **f**, Dynamics of the 50S ribosomal L1 stalk monitored by single-molecule fluorescence resonance energy transfer (smFRET). Representative smFRET trace (top) and histogram (bottom left) of the L1 stalk dynamically sampling open and closed conformations in A- and P-site tRNA-bound ribosome complexes. Translocation by EF-G and tRNA occupation of the E- and P-sites causes the L1 stalk conformation to shift dramatically (bottom right). Figure modified, with permission, from ref. 100.

tRNA–RNP complexes show that binding is often accompanied by significant conformational changes, which range from the reorientation of helical domains to finer changes in local structure, all of which optimize intermolecular interactions[68] (Fig. 4a).

Ordering RNP assembly

RNA tertiary conformational changes that are induced by successive protein-binding events are thought to help direct the order of assembly of complex RNP machines, including the 30S ribosome[69,70], the signal recognition particle[71] and telomerase[72]. For example, the binding of ribosomal protein S15 to 16S rRNA initiates the ordered assembly of the central domain in the 30S ribosomal subunit[73], and leads to a change in the orientation of helical domains that favours the binding of ribosomal proteins S6 and S18 (ref. 74) (Fig. 4b). Premature binding of S6 and S18 to the unbound 16S rRNA may be disfavoured, in part, because of the entropic penalty that is associated with the partial freezing-out of interhelical motions. Even in the simpler telomerase RNP (consisting of one RNA and two protein components), the binding of the first protein p65 induces a conformational change in the RNA that facilitates the binding of telomerase reverse transcriptase, thereby ordering assembly[72].

Assembly can also involve coupled protein binding that induces changes in both RNA secondary and tertiary structure. For example, coupled binding of the maturase and Mrs1 protein cofactors to the RNA of the bI3 group-I intron RNP stabilizes both the native tertiary contacts and induces a reorganization of a non-native intermediate secondary structure[75]. Although both Mrs1 dimers and maturase can independently bind and stabilize portions of the bI3 tertiary structure, binding by both proteins is required to induce the secondary structure rearrangement and assembly to the native, active state.

Ribozyme catalysis

Tertiary conformational transitions involving large changes in the orientation of helical arms are often observed in small ribozymes, such as the hairpin and HDV, and are thought to be important for the transition between the different steps of the catalytic cycles. Typically, an undocked (inactive) conformation binds the substrate, promoting the transition into a docked (active) conformation, which is required for catalysis. After catalysis, another undocking transition allows the release of the product (Fig. 4c). The importance of these motions is demonstrated by the fact that the junction motions can accelerate the rate of folding of the active conformation[76]. Similarly, large hinge-like motions of the J2a/b bulge in human telomerase have been proposed to help with dynamic telomere repeat synthesis[77]. A more exceptional example is the *Tetrahymena* group-I ribozyme that has been shown to interconvert between alternative tertiary conformations, which have a range of substrate binding affinities but similar enzymatic activities[78]. The rates of interconversion between these states are slower than the rate of catalysis, implying the existence of multiple native states. Such long-lived heterogeneities have been observed in the tertiary folds of many other RNAs, although some of these may be the result of RNA purification side-products[79]. The atomic level structural differences between these species and the source of the severe heterogeneity are still unknown but they may constitute yet another mechanism used by RNA to define a narrow set of differentiated conformations and this should be an exciting topic for future research.

Protein synthesis

Perhaps the best example of the cell manipulating the intrinsic dynamic landscape of RNA to achieve a desired biological outcome is ribosome catalysis. Large-scale ratcheting motions are required for translation. The small and large subunits reorient with respect to one another through numerous structural intermediates that are driven by changes in the conformation of both the ribosomal RNAs and proteins[80–84] (Fig. 4d). Data strongly indicate that all of these intermediates are relatively low-lying energy states that readily interconvert, which has been highlighted by the ability of the ribosome to spontaneously undergo full tRNA retrotranslocation[84,85] (Fig. 4e). This has led to a 'Brownian machine' model of the ribosome, where the ribosome's functionality is derived in part by its ability to harness thermally driven equilibrium fluctuations and bias them to promote the translation process[22] (Fig. 4f).

The cell combines these intrinsic ribosome dynamics with numerous effectors to achieve tight control over the complex transactions that are required by translation. One such transaction is the selection and proofreading of incoming tRNAs that are responsible for the ribosome's remarkable ability to consistently discriminate between cognate and near- or non-cognate tRNAs, in which small differences between the minihelices of incorrect and correct anticodon–codon pairs will lead to tRNA accommodation or rejection. Here, the formation of a cognate minihelix results in a kinked tRNA structure and triggers a 30S 'domain closure' motion[86–88]. This stabilizes tRNA–ribosome interactions and in turn promotes conformational rearrangements in the EF-Tu protein of the EF-Tu•GTP-tRNA ternary complex that delivered tRNA to the ribosome; this results in EF-Tu•GTP hydrolysis, release of tRNA from EF-Tu and initial tRNA selection[89,90]. The second proofreading step that follows EF-Tu dissociation is thought to be driven by relaxation of the kinked tRNA. In cognate tRNAs, the strong interactions between the codon and the anticodon cause a bias of tRNA relaxation towards a conformation that is fully accommodated within the A-site. However, for near-cognate tRNAs, which have weak codon–anticodon interactions, the relaxation of the kinked tRNA can occur through other pathways that lead to rejection[91,92]. Following tRNA accommodation, other factors, including EF-G[93], other initiation factors[94], recycling factors[95], release factors[96], and even the identity and acylation state of the tRNA occupying the neighbouring ribosomal P-site[97], act on the translation process, manipulating the ribosome's dynamic landscape to drive efficient synthesis of the mRNA-encoded protein.

Owing to the overwhelming complexity of the ribosome, the mechanisms and atomic level details of the many conformational transitions involved in the translation process remain unclear. Among these unresolved questions are how the ribosome's RNA and protein components cooperate to confer dynamic specificity and robustness on ribosome dynamics[98]. Research into this process is another exciting area of future study, and we can confidently predict that this will be yet another biological system shown to rely heavily on the virtuosity of RNA dynamics.

Outlook

The conventional view that one sequence codes for one structure and one function is being replaced by a dynamic view of RNA as a pre-existing superposition of conformational states that can be resolved into a directed and synchronized motion by dedicated cellular machinery, leading to a broad range of functional outcomes. This makes it all the more important to study RNA dynamics within the complex *in vivo* environment of living cells, an important goal for the future. We also need to increase our basic understanding of RNA dynamic behaviour, even within the simpler *in vitro* environment. It is remarkable that, even for well-studied molecules such as tRNA, there is very little experimental data available regarding the equilibrium fluctuations in tRNA at the atomic level; the same is also true for catalytically important motions in ribozymes. Similarly, little is known about the structure and dynamics of large RNAs, such as eukaryotic mRNAs. This will require the combined development of computational and experimental tools to move towards developing atomic-level movies of RNA in dynamic action within living cells as well as a better predictive understanding of RNA dynamic behaviour. In the meantime, great advances can be made by simply embracing this new dynamic view of RNA and always being on the lookout for another myoglobin. ■

1. Kendrew, J. C. *et al.* A three-dimensional model of the myoglobin molecule obtained by X-ray analysis. *Nature* **181,** 662–666 (1958).
2. Rould, M. A., Perona, J. J., Söll, D. & Steitz, T. A. Structure of *E. coli* glutaminyl-tRNA synthetase complexed with tRNA(Gln) and ATP at 2.8 Å resolution. *Science* **246,** 1135–1142 (1989).
3. Pley, H. W., Flaherty, K. M. & McKay, D. B. Three-dimensional structure of a hammerhead ribozyme. *Nature* **372,** 68–74 (1994).
4. Scott, W. G., Finch, J. T. & Klug, A. The crystal structure of an all-RNA hammerhead ribozyme: a proposed mechanism for RNA catalytic cleavage. *Cell* **81,** 991–1002 (1995).
5. Wang, S., Karbstein, K., Peracchi, A., Beigelman, L. & Herschlag, D. Identification of the hammerhead ribozyme metal ion binding site responsible for rescue of the deleterious effect of a cleavage site phosphorothioate. *Biochemistry* **38,** 14363–14378 (1999).
6. Boehr, D. D., Nussinov, R. & Wright, P. E. The role of dynamic conformational ensembles in biomolecular recognition. *Nature Chem. Biol.* **5,** 789–796 (2009).
7. Al-Hashimi, H. M. & Walter, N. G. RNA dynamics: it is about time. *Curr. Opin. Struct. Biol.* **18,** 321–329 (2008).
8. Frauenfelder, H., Sligar, S. G. & Wolynes, P. G. The energy landscapes and motions of proteins. *Science* **254,** 1598–1603 (1991).
9. Cruz, J. A. & Westhof, E. The dynamic landscapes of RNA architecture. *Cell* **136,** 604–609 (2009).
10. Bailor, M. H., Mustoe, A. M., Brooks, C. L. 3rd & Al-Hashimi, H. M. Topological constraints: using RNA secondary structure to model 3D conformation, folding pathways, and dynamic adaptation. *Curr. Opin. Struct. Biol.* **21,** 296–305 (2011).
11. Schultes, E. A., Spasic, A., Mohanty, U. & Bartel, D. P. Compact and ordered collapse of randomly generated RNA sequences. *Nature Struct. Mol. Biol.* **12,** 1130–1136 (2005).
12. Schultes, E. A., Hraber, P. T. & LaBean, T. H. Estimating the contributions of selection and self-organization in RNA secondary structure. *J. Mol. Evol.* **49,** 76–83 (1999).
13. Fürtig, B., Wenter, P., Pitsch, S. & Schwalbe, H. Probing mechanism and transition state of RNA refolding. *ACS Chem. Biol.* **5,** 753–765 (2010).
14. Bailor, M. H., Sun, X. & Al-Hashimi, H. M. Topology links RNA secondary structure with global conformation, dynamics, and adaptation. *Science* **327,** 202–206 (2010).
This article reports the simple topological constraints that are governed by steric and stereochemical forces severely restrict the allowed orientation of helices across two-way junctions.
15. Mustoe, A. M., Bailor, M. H., Teixeira, R. M., Brooks, C. L. 3rd & Al-Hashimi, H. M. New insights into the fundamental role of topological constraints as a determinant of two-way junction conformation. *Nucleic Acids Res.* **40,** 892–904 (2012).
16. Chu, V. B. *et al.* Do conformational biases of simple helical junctions influence RNA folding stability and specificity? *RNA* **15,** 2195–2205 (2009).
17. Venditti, V., Clos, L. 2nd, Niccolai, N. & Butcher, S. E. Minimum-energy path for a U6 RNA conformational change involving protonation, base-pair rearrangement and base flipping. *J. Mol. Biol.* **391,** 894–905 (2009).
18. Fourmy, D., Yoshizawa, S. & Puglisi, J. D. Paromomycin binding induces a local conformational change in the A-site of 16S rRNA. *J. Mol. Biol.* **277,** 333–345 (1998).
19. Le, S. Y., Zhang, K. & Maizel, J. V. Jr. RNA molecules with structure dependent functions are uniquely folded. *Nucleic Acids Res.* **30,** 3574–3582 (2002).
20. Stelzer, A. C., Kratz, J. D., Zhang, Q. & Al-Hashimi, H. M. RNA dynamics by design: biasing ensembles towards the ligand-bound state. *Angew. Chem. Int. Ed. Engl.* **49,** 5731–5733 (2010).
21. Shankar, N. *et al.* NMR reveals the absence of hydrogen bonding in adjacent UU and AG mismatches in an isolated internal loop from ribosomal RNA. *Biochemistry* **46,** 12665–12678 (2007).
22. Frank, J. & Gonzalez, R. L., Jr. Structure and dynamics of a processive Brownian motor: the translating ribosome. *Annu. Rev. Biochem.* **79,** 381–412 (2010).
23. Haller, A., Souliere, M. F. & Micura, R. The dynamic nature of RNA as key to understanding riboswitch mechanisms. *Acc. Chem. Res.* **44,** 1339–1348 (2011).
24. Paukstelis, P. J., Chen, J. H., Chase, E., Lambowitz, A. M. & Golden, B. L. Structure of a tyrosyl-tRNA synthetase splicing factor bound to a group I intron RNA. *Nature* **451,** 94–97 (2008).
25. Puglisi, J. D., Tan, R., Calnan, B. J., Frankel, A. D. & Williamson, J. R. Conformation of the TAR RNA-arginine complex by NMR spectroscopy. *Science* **257,** 76–80 (1992).
26. Orr, J. W., Hagerman, P. J. & Williamson, J. R. Protein and Mg^{2+}-induced conformational changes in the S15 binding site of 16S ribosomal RNA. *J. Mol. Biol.* **275,** 453–464 (1998).
27. Turner, B., Melcher, S. E., Wilson, T. J., Norman, D. G. & Lilley, D. M. Induced fit of RNA on binding the L7Ae protein to the kink-turn motif. *RNA* **11,** 1192–1200 (2005).
28. Falb, M., Amata, I., Gabel, F., Simon, B. & Carlomagno, T. Structure of the K-turn U4 RNA: a combined NMR and SANS study. *Nucleic Acids Res.* **38,** 6274–6285 (2010).
29. Kim, H. D. *et al.* Mg^{2+}-dependent conformational change of RNA studied by fluorescence correlation and FRET on immobilized single molecules. *Proc. Natl Acad. Sci. USA* **99,** 4284–4289 (2002).
30. Zacharias, M. & Hagerman, P. J. The influence of symmetric internal loops on the flexibility of RNA. *J. Mol. Biol.* **257,** 276–289 (1996).
31. Zhang, Q., Stelzer, A. C., Fisher, C. K. & Al-Hashimi, H. M. Visualizing spatially correlated dynamics that directs RNA conformational transitions. *Nature* **450,** 1263–1267 (2007).
32. Shajani, Z., Drobny, G. & Varani, G. Binding of U1A protein changes RNA dynamics as observed by ^{13}C NMR relaxation studies. *Biochemistry* **46,** 5875–5883 (2007).
33. Bokinsky, G. *et al.* Two distinct binding modes of a protein cofactor with its target RNA. *J. Mol. Biol.* **361,** 771–784 (2006).
34. Bardaro, M. F. Jr., Shajani, Z., Patora-Komisarska, K., Robinson, J. A. & Varani, G. How binding of small molecule and peptide ligands to HIV-1 TAR alters the RNA motional landscape. *Nucleic Acids Res.* **37,** 1529–1540 (2009).
35. Herschlag, D., Khosla, M., Tsuchihashi, Z. & Karpel, R. L. An RNA chaperone activity of non-specific RNA binding proteins in hammerhead ribozyme catalysis. *EMBO J.* **13,** 2913–2924 (1994).
36. Pyle, A. M. & Green, J. B. RNA folding. *Curr. Opin. Struct. Biol.* **5,** 303–310 (1995).
37. Treiber, D.K. & Williamson, J.R. Beyond kinetic traps in RNA folding. *Curr. Opin. Struct. Biol.* **11,** 309–314 (2001).
38. Hirling, H., Scheffner, M., Restle, T. & Stahl, H. RNA helicase activity associated with the human p68 protein. *Nature* **339,** 562–564 (1989).
39. Yang, Q. & Jankowsky, E. ATP- and ADP-dependent modulation of RNA unwinding and strand annealing activities by the DEAD-box protein DED1. *Biochemistry* **44,** 13591–13601 (2005).
40. Will, C. L. & Lührmann, R. Spliceosome structure and function. *Cold Spring Harb. Perspect. Biol.* **3,** a003707 (2011).
41. Kosowski, T. R., Keys, H. R., Quan, T. K. & Ruby, S. W. DExD/H-box Prp5 protein is in the spliceosome during most of the splicing cycle. *RNA* **15,** 1345–1362 (2009).
42. Maeder, C., Kutach, A. K. & Guthrie, C. ATP-dependent unwinding of U4/U6 snRNAs by the Brr2 helicase requires the C terminus of Prp8. *Nature Struct. Mol. Biol.* **16,** 42–48 (2009).
43. Schwer, B. A conformational rearrangement in the spliceosome sets the stage for Prp22-dependent mRNA release. *Mol. Cell* **30,** 743–754 (2008).
44. Bhaskaran, H. & Russell, R. Kinetic redistribution of native and misfolded RNAs by a DEAD-box chaperone. *Nature* **449,** 1014–1018 (2007).
45. Winkler, W., Nahvi, A. & Breaker, R. R. Thiamine derivatives bind messenger RNAs directly to regulate bacterial gene expression. *Nature* **419,** 952–956 (2002).
This article reports the discovery of an RNA switch in the 5′ untranslated region of bacterial mRNA that regulates gene expression in response to ligands without assistance from proteins.
46. Cromie, M. J., Shi, Y., Latifi, T. & Groisman, E. A. An RNA sensor for intracellular Mg^{2+}. *Cell* **125,** 71–84 (2006).
47. Nechooshtan, G., Elgrably-Weiss, M., Sheaffer, A., Westhof, E. & Altuvia, S. A pH-responsive riboregulator. *Genes Dev.* **23,** 2650–2662 (2009).
48. Greenleaf, W. J., Frieda, K. L., Foster, D. A. Woodside, M. T. & Block, S. M. Direct observation of hierarchical folding in single riboswitch aptamers. *Science* **319,** 630–633 (2008).
49. Mandal, M. *et al.* A glycine-dependent riboswitch that uses cooperative binding to control gene expression. *Science* **306,** 275–279 (2004).
50. Sudarsan, N. *et al.* Tandem riboswitch architectures exhibit complex gene control functions. *Science* **314,** 300–304 (2006).
51. Lee, E. R., Baker, J. L., Weinberg, Z., Sudarsan, N. & Breaker, R. R. An allosteric self-splicing ribozyme triggered by a bacterial second messenger. *Science* **329,** 845–848 (2010).
52. Ferre-D'Amare, A. R., Zhou, K. & Doudna, J. A. Crystal structure of a hepatitis delta virus ribozyme. *Nature* **395,** 567–574 (1998).
53. Ke, A., Zhou, K., Ding, F., Cate, J. H. D. & Doudna, J. A. A conformational switch controls hepatitis delta virus ribozyme catalysis. *Nature* **429,** 201–205 (2004).
This article reports a significant local conformational change in the active site of the HDV ribozyme is observed post-cleavage and is associated with ejection of the substrate and a catalytically critical divalent metal ion.
54. Harris, D. A., Rueda, D. & Walter, N. G. Local conformational changes in the catalytic core of the *trans*-acting hepatitis delta virus ribozyme accompany catalysis. *Biochemistry* **41,** 12051–12061 (2002).
55. Lamanna, A. C. & Karbstein, K. An RNA conformational switch regulates pre-18S rRNA cleavage. *J. Mol. Biol.* **405,** 3–17 (2011).
56. Nocker, A. *et al.* A mRNA-based thermosensor controls expression of rhizobial heat shock genes. *Nucleic Acids Res.* **29,** 4800–4807 (2001).
57. Johansson, J. *et al.* An RNA thermosensor controls expression of virulence genes in *Listeria monocytogenes*. *Cell* **110,** 551–561 (2002).
58. Watts, J. M. et al. Architecture and secondary structure of an entire HIV-1 RNA genome. *Nature* **460,** 711–716 (2009).
59. Grundy, F. J., Winkler, W. C. & Henkin, T. M. tRNA-mediated transcription antitermination *in vitro*: codon-anticodon pairing independent of the ribosome. *Proc. Natl Acad. Sci. USA* **99,** 11121–11126 (2002).
60. Babitzke, P. & Yanofsky, C. Reconstitution of *Bacillus subtilis trp* attenuation *in vitro* with TRAP, the *trp* RNA-binding attenuation protein. *Proc. Natl Acad. Sci. USA* **90,** 133–137 (1993).
61. Diaz-Toledano, R., Ariza-Mateos, A., Birk, A., Martinez-Garcia, B. & Gomez, J. *In vitro* characterization of a miR-122-sensitive double-helical switch element in the 5′ region of hepatitis C virus RNA. *Nucleic Acids Res.* **37,** 5498–5510 (2009).
62. Ray, P. S. *et al.* A stress-responsive RNA switch regulates *VEGFA* expression. *Nature* **457,** 915–919 (2009).
This article reports that the 3′ untranslated region of human *VEGFA* mRNA undergoes a binary conformational switch in response to inflammatory and hypoxic protein stress signals to regulate *VEGFA* expression.
63. Cheah, M. T., Wachter, A., Sudarsan, N. & Breaker, R. R. Control of alternative RNA splicing and gene expression by eukaryotic riboswitches. *Nature* **447,** 497–500 (2007).

This article reports a secondary structural change in a eukaryotic thiamine pyrophosphate riboswitch regulates gene expression through the control of alternative splicing.
64. Kedde, M. *et al.* A Pumilio-induced RNA structure switch in p27-3′ untranslated region controls miR-221 and miR-222 accessibility. *Nature Cell Biol.* **12,** 1014–1020 (2010).
65. Casey, J. L. Control of ADAR1 editing of hepatitis delta virus RNAs. *Curr. Top. Microbiol. Immunol.* **353,** 123–143 (2012).
66. Abbink, T. E., Ooms, M., Haasnoot, P. C. & Berkhout, B. The HIV-1 leader RNA conformational switch regulates RNA dimerization but does not regulate mRNA translation. *Biochemistry* **44,** 9058–9066 (2005).
67. Miyazaki, Y. *et al.* An RNA structural switch regulates diploid genome packaging by Moloney murine leukemia virus. *J. Mol. Biol.* **396,** 141–152 (2010).
This article reports that dimerization of the 5′ untranslated region of the Moloney murine leukaemia virus results in a secondary structural change that promotes genome packaging.
68. Giege, R. Toward a more complete view of tRNA biology. *Nature Struct. Mol. Biol.* **15,** 1007–1014 (2008).
69. Mulder, A. M. *et al.* Visualizing ribosome biogenesis: parallel assembly pathways for the 30S subunit. *Science* **330,** 673–677 (2010).
70. Adilakshmi, T., Bellur, D. L. & Woodson, S. A. Concurrent nucleation of 16S folding and induced fit in 30S ribosome assembly. *Nature* **455,** 1268–1272 (2008).
71. Menichelli, E., Isel, C., Oubridge, C. & Nagai, K. Protein-induced conformational changes of RNA during the assembly of human signal recognition particle. *J. Mol. Biol.* **367,** 187–203 (2007).
72. Stone, M. D. *et al.* Stepwise protein-mediated RNA folding directs assembly of telomerase ribonucleoprotein. *Nature* **446,** 458–461 (2007).
73. Held, W. A., Ballou, B., Mizushima, S. & Nomura, M. Assembly mapping of 30S ribosomal proteins from *Escherichia coli*. Further studies. *J. Biol. Chem.* **249,** 3103–3111 (1974).
74. Agalarov, S. C., Prasad, G. S., Funke, P. M., Stout, C. D. & Williamson, J. R. Structure of the S15,S6,S18-rRNA complex: assembly of the 30S ribosome central domain. *Science* **288,** 107–112 (2000).
75. Duncan, C. D. & Weeks, K. M. Nonhierarchical ribonucleoprotein assembly suggests a strain-propagation model for protein-facilitated RNA folding. *Biochemistry* **49,** 5418–5425 (2010).
76. Wilson, T. J., Nahas, M., Ha, T. & Lilley, D. M. Folding and catalysis of the hairpin ribozyme. *Biochem. Soc. Trans.* **33,** 461–465 (2005).
77. Zhang, Q., Kim, N. K., Peterson, R. D., Wang, Z. & Feigon, J. Structurally conserved five nucleotide bulge determines the overall topology of the core domain of human telomerase RNA. *Proc. Natl Acad. Sci. USA* **107,** 18761–18768 (2010).
78. Solomatin, S. V., Greenfeld, M., Chu, S. & Herschlag, D. Multiple native states reveal persistent ruggedness of an RNA folding landscape. *Nature* **463,** 681–684 (2010).
This article reports the observation of slowly interconverting catalytically active states in a ribozyme, thereby establishing the coexistence of multiple native states.
79. Greenfeld, M., Solomatin, S. V. & Herschlag, D. Removal of covalent heterogeneity reveals simple folding behavior for P4–P6 RNA. *J. Biol. Chem.* **286,** 19872–19879 (2011).
80. Frank, J. & Agrawal, R. K. A ratchet-like inter-subunit reorganization of the ribosome during translocation. *Nature* **406,** 318–322 (2000).
81. Valle, M. *et al.* Locking and unlocking of ribosomal motions. *Cell* **114,** 123–134 (2003).
82. Zhang, W., Dunkle, J. A. & Cate, J. H. Structures of the ribosome in intermediate states of ratcheting. *Science* **325,** 1014–1017 (2009).
83. Ratje, A. H. *et al.* Head swivel on the ribosome facilitates translocation by means of intra-subunit tRNA hybrid sites. *Nature* **468,** 713–716 (2010).
84. Fischer, N., Konevega, A. L. Wintermeyer, W., Rodnina, M. V. & Stark, H. Ribosome dynamics and tRNA movement by time-resolved electron cryomicroscopy. *Nature* **466,** 329–333 (2010).
This article demonstrates the cryo-electron microscopy observation of thermally driven tRNA retrotranslocation on the ribosome.
85. Shoji, S., Walker, S. E. & Fredrick, K. Reverse translocation of tRNA in the ribosome. *Mol. Cell* **24,** 931–942 (2006).
86. Ogle, J. M., Murphy, F. V., Tarry, M. J. & Ramakrishnan, V. Selection of tRNA by the ribosome requires a transition from an open to a closed form. *Cell* **111,** 721–732 (2002).
87. Valle, M. *et al.* Incorporation of aminoacyl-tRNA into the ribosome as seen by cryo-electron microscopy. *Nature Struct. Biol.* **10,** 899–906 (2003).
88. Lee, T. H., Blanchard, S. C., Kim, H. D., Puglisi, J. D. & Chu, S. The role of fluctuations in tRNA selection by the ribosome. *Proc. Natl Acad. Sci. USA* **104,** 13661–13665 (2007).
89. Schmeing, T. M. *et al.* The crystal structure of the ribosome bound to EF-Tu and aminoacyl-tRNA. *Science* **326,** 688–694 (2009).
90. Voorhees, R. M., Schmeing, T. M., Kelley, A. C. & Ramakrishnan, V. The mechanism for activation of GTP hydrolysis on the ribosome. *Science* **330,** 835–838 (2010).
91. Pape, T., Wintermeyer, W. & Rodnina, M. V. Conformational switch in the decoding region of 16S rRNA during aminoacyl-tRNA selection on the ribosome. *Nature Struct. Mol. Biol.* **7,** 104–107 (2000).
92. Blanchard, S. C., Gonzalez, R. L., Kim, H. D., Chu, S. & Puglisi, J. D. tRNA selection and kinetic proofreading in translation. *Nature Struct. Mol. Biol.* **11,** 1008–1014 (2004).
This important single-molecule FRET study directly observes the dynamics of tRNA initial selection and proofreading by the ribosome.
93. Fei, J. *et al.*, Allosteric collaboration between elongation factor G and the ribosomal L1 stalk directs tRNA movements during translation. *Proc. Natl Acad. Sci. USA* **106,** 15702–15707 (2009).
94. Blaha, G., Stanley, R. E. & Steitz, T. A. Formation of the first peptide bond: the structure of EF-P bound to the 70S ribosome. *Science* **325,** 966–970 (2009).
95. Dunkle, J. A. *et al.* Structures of the bacterial ribosome in classical and hybrid states of tRNA binding. *Science* **332,** 981–984 (2011).
96. Laurberg, M. *et al.* Structural basis for translation termination on the 70S ribosome. *Nature* **454,** 852–857 (2008).
97. Cornish, P. V., Ermolenko, D. N., Noller, H. F. & Ha, T. Spontaneous intersubunit rotation in single ribosomes. *Mol. Cell* **30,** 578–588 (2008).
98. Tama, F., Valle, M., Frank, J. & Brooks, C. L 3rd. Dynamic reorganization of the functionally active ribosome explored by normal mode analysis and cryo-electron microscopy. *Proc. Natl Acad. Sci. USA* **100,** 9319–9323 (2003).
99. Green, N. J., Grundy, F. J. & Henkin, T. M. The T box mechanism: tRNA as a regulatory molecule. *FEBS Lett.* **584,** 318–324 (2010).
100. Cornish, P. V. *et al.* Following movement of the L1 stalk between three functional states in single ribosomes. *Proc. Natl Acad. Sci. USA* **106,** 2571–2576 (2009).

Supplementary Information is linked to the online version of the paper at www.nature.com/nature.

Acknowledgements E.A.D. and J.C. contributed equally to this Review. We thank C. Eichhorn and Q. Zhang for their input and assistance in the preparation of figures, and S. Butcher and S. Serganov for their comments on this Review. A.M.M. is supported by an NSF graduate research fellowship. The authors gratefully acknowledge the Michigan Economic Development Cooperation and the Michigan Technology Tri-Corridor for their support in the purchase of a 600 MHz spectrometer. This work was supported by the US National Institutes of Health (R01 AI066975 and R01 GM089846) and the US National Science Foundation (NSF Career Award CHE-0918817).

Author Information Reprints and permissions information is available at www.nature.com/reprints. The authors declare no competing financial interests. Readers are welcomed to comment on the online version of this article at www.nature.com/nature. Correspondence should be addressed to author H.M.A.H. (hashimi@umich.edu).